

Production of ^{55}Co via the $^{54}\text{Fe}(d, n)$ -process and excitation functions of $^{54}\text{Fe}(d, t)^{53}\text{Fe}$ and $^{54}\text{Fe}(d, \alpha)^{52\text{m}}\text{Mn}$ reactions from threshold up to 13.8 MeV

By M. R. Zaman[†], S. Spellerberg and S. M. Qaim*

Institut für Nuklearchemie, Forschungszentrum Jülich GmbH, D-52425 Jülich, Germany

(Received February 4, 2002; accepted in revised form July 3, 2002)

*^{55}Co production / Yield and purity / Nuclear reaction /
Excitation function / Isomeric cross section ratio*

Summary. For production of the medically interesting β^+ -emitter ^{55}Co ($T_{1/2} = 17.6$ h) via the $^{54}\text{Fe}(d, n)$ -reaction, 91.6% enriched $^{54}\text{Fe}_2\text{O}_3$, mixed with Al powder, was pressed to a pellet which could be irradiated with 14 MeV deuterons at 4 μA in a water-cooled target system. A separation method was developed which led to > 99.9% pure ^{55}Co and allowed a recovery of the enriched target material. For a target thickness of $E_d = 12.6 \rightarrow 5$ MeV, the experimental thick target yield of ^{55}Co after chemical separation amounted to about 13 MBq/ $\mu\text{A}\cdot\text{h}$, which is about 60% of the theoretical value. In a 3 h irradiation at 4 μA , the batch yield of ^{55}Co achieved was 160 MBq (4.3 mCi). An 8 h irradiation could lead to a batch yield of about 400 MBq. The $^{54}\text{Fe}(d, n)$ reaction leads to the highest purity ^{55}Co but it is essential that the isotopic enrichment of the target is not less than 90%. In addition to the production work, cross sections were measured for the $^{54}\text{Fe}(d, t)^{53}\text{Fe}$ and $^{54}\text{Fe}(d, \alpha)^{52\text{m}}\text{Mn}$ reactions using the standard stacked-foil technique and high-resolution γ -ray spectrometry. The cross section ratio for the isomeric pair $^{52\text{m,g}}\text{Mn}$ is discussed in terms of the spins of the two states involved and the increasing projectile energy.

1. Introduction

The radionuclide cobalt-55 ($T_{1/2} = 17.6$ h; $E_{\beta^+} = 1.5$ MeV; $I_{\beta^+} = 77\%$) is an important β^+ -emitting radioisotope. It has found application in labelling bleomycin, monoclonal antibodies and perfusion markers for some cardiac and cerebral studies [cf. 1–5] using positron emission tomography (PET). For its production, three routes have been commonly used, namely $^{56}\text{Fe}(p, 2n)^{55}\text{Co}$, $^{58}\text{Ni}(p, \alpha)^{55}\text{Co}$ and $^{54}\text{Fe}(d, n)^{55}\text{Co}$. A summary of the calculated ^{55}Co yields and impurity levels is given in Table 1. The $^{56}\text{Fe}(p, 2n)^{55}\text{Co}$ reaction has the highest yield but the level of the ^{56}Co impurity ($T_{1/2} = 78.8$ d) is high [cf. 1–4]. The $^{58}\text{Ni}(p, \alpha)^{55}\text{Co}$ process has been well developed [cf. 5–7] but, even using highly

enriched ^{58}Ni as target material, about 0.5% ^{57}Co impurity ($T_{1/2} = 271.3$ d) cannot be avoided [7]. The $^{54}\text{Fe}(d, n)^{55}\text{Co}$ reaction leads to the highest purity product, provided highly enriched ^{54}Fe is used as target material [8, 9]. A medium-scale production of ^{55}Co via this route has been described [8]. We investigated this reaction earlier [9] from the viewpoint of nuclear data. Now we describe some work on targetry and chemical processing. Cross sections for the competing (d, t) and (d, α) reactions on ^{54}Fe are also reported.

2. Production of ^{55}Co

2.1 Targetry

About 125 mg of $^{54}\text{Fe}_2\text{O}_3$ (stated isotopic composition: $^{54}\text{Fe} = 91.6\%$, $^{56}\text{Fe} = 8.20\%$, $^{57}\text{Fe} = 0.2\%$; stated chemical impurities: Mg, Al, Cl, Co, Ni, Cu, Sb (< 50 ppm); Si, Ca, Cr (< 300 ppm), supplied by Chemotrade GmbH, Germany/Russia) was thoroughly mixed with 45 mg of fine Al powder (> 98%, < 160 μm , FLUKA, Germany) in a mortar, and then pressed to a pellet of 1.3 cm diameter at 10 tons/ cm^2 (23.8 MPa). Addition of Al was necessary to be able to press $^{54}\text{Fe}_2\text{O}_3$ to a pellet. The thickness of the pellet amounted to about 250 μm . The pellet was placed in the groove of a Cu-target holder and covered by a 100 μm Cu foil. The target holder was then attached to an irradiation system which was cooled from three sides by flowing water at 13 °C. This target arrangement [cf. 10] could withstand an irradiation with 14 MeV deuterons at 4 μA . The effective deuteron energy in the target pellet was 12.6 \rightarrow 5 MeV.

2.2 Chemical processing

After irradiation the pellet was dissolved in 4 mL of conc. HCl and 2 mL of H_2O_2 . The solution was evaporated to dryness to remove H_2O_2 , the residue was taken up in 5 mL of conc. HCl and ^{54}Fe was removed by extraction with two 10 mL portions of diethyl ether saturated with conc. HCl. The aqueous solution was evaporated to dryness slowly to remove traces of ether. The residue was taken up in 10 mL of conc. HCl. It contained radiocobalt and radiomanganese at the no-carrier-added level and Al in macroquantities. It was

* Author for correspondence (E-mail: s.m.qaim@fz-juelich.de).

[†] Guest scientist from the Department of Applied Chemistry and Chemical Technology, Rajshahi University, Rajshahi-6205, Bangladesh

Table 1. Calculated yields and impurity levels (at EOB) in the production of ^{55}Co via common routes.

Production route	Energy range [MeV]	^{55}Co yield [MBq/ $\mu\text{A}\cdot\text{h}$]	Impurity (%)	Major reference
$^{56}\text{Fe}(p, 2n)^{55}\text{Co}$	38 \rightarrow 14	163	^{56}Co (1.6)	1
$^{58}\text{Ni}(p, \alpha)^{55}\text{Co}^a$	15 \rightarrow 7	14	^{57}Co (0.5)	6
$^{54}\text{Fe}(d, n)^{55}\text{Co}^a$	10 \rightarrow 5	32	$^{56,57}\text{Co}$ (< 0.01)	9

a: Using 99.9% enriched target material.

then transferred to a column ($\varnothing = 2.0$ cm, height = 10 cm) filled with the anion-exchange resin Dowex 1 \times 8, chloride form, 100–200 mesh (FLUKA). The column was conditioned with 10 mL of conc. HCl, then eluted with 10 mL of 6 M HCl whereby radiomanganese was quantitatively removed. Thereafter elution was done with 60 mL of 4 M HCl; radiocobalt was removed from the column and existed in about 40 mL of the elute. Al remained on the column. The fractions containing ^{52}Mn and ^{55}Co were separately collected and concentrated by evaporation. ^{55}Co was finally obtained as $^{55}\text{CoCl}_2$ in 2 mL of 1 M HCl. The recovery of the enriched ^{54}Fe from solution in diethyl ether was done by a careful removal of the ether at 35–40 °C, redissolution in conc. HCl, precipitation as $^{54}\text{Fe}(\text{OH})_3$ and conversion to $^{54}\text{Fe}_2\text{O}_3$ by heating at 800 °C. In this form it could be used again as target material. The recovery yield was > 80%.

2.3 Yield and purity

A 3 h irradiation of the above mentioned target pellet at 4 μA led to about 160 MBq of the separated ^{55}Co extrapolated to the end of bombardment (EOB). The experimental thick target yield was thus about 13 MBq/ $\mu\text{A}\cdot\text{h}$. This value is about 60% of the theoretical value and is rather good. The target cannot withstand beam currents above 4 μA but the irradiation time could be extended. Thus an 8 h irradiation would lead to about 400 MBq of ^{55}Co . Our yields are comparable to those reported in another work [8] which made use of a different target system.

The radionuclidic purity of the separated radiocobalt was determined via high-resolution HPGe detector γ -ray spectrometry. The composition was found to be: ^{55}Co (> 99.9%), ^{56}Co (< 0.02%), ^{57}Co (0.06%). The level of ^{52}Mn was < 0.01%. These results are in general agreement with the production data reported by Sharma *et al.* [8] using 87.9% enriched ^{54}Fe targets. The $^{56,57}\text{Co}$ impurities are due to the presence of ^{56}Fe and ^{57}Fe in the enriched ^{54}Fe target material. The radionuclidic purity of ^{55}Co produced via the $^{54}\text{Fe}(d, n)$ process using 91.6% enriched ^{54}Fe is not as good as from the 99.85% enriched ^{54}Fe used earlier [9], but it is still very good.

The chemical purity of the separated radiocobalt was checked by ICP-OES. The amounts of Fe, Mn, Ni, Cr and Mg were found to be < 1 ppm. The amount of Al was estimated via neutron activation analysis using the nuclear reaction $^{27}\text{Al}(n, p)^{27}\text{Mg}$ ($T_{1/2} = 9.5$ min) with 14 MeV $d(\text{Be})$ neutrons. An upper limit for the Al content in the separated radiocobalt was placed at 50 ppm.

2.4 Prospects of availability and use of ^{55}Co

The $^{56}\text{Fe}(p, 2n)^{55}\text{Co}$ reaction gives the highest ^{55}Co yield and, in spite of the rather high ^{56}Co impurity, the product has

been used in a few limited brain studies on patients [cf. 4]. The use of $^{\text{nat}}\text{Fe}$ as target material makes targetry easy and ^{55}Co quantities of about 2 GBq can be conveniently produced. However, the ^{56}Co impurity limits the use of the product only over short periods, *i.e.* for fast metabolic processes. The $^{58}\text{Ni}(p, \alpha)^{55}\text{Co}$ process is technically well developed [cf. 7] but the yield of ^{55}Co is low and the level of ^{57}Co impurity (0.5%) is of some concern. It can thus probably be used only in animal experiments. The radionuclidic purity of ^{55}Co produced via the $^{54}\text{Fe}(d, n)$ reaction using 91.6% enriched ^{54}Fe is still superior to the products from the other two routes. Based on the cross sections for the $^{56}\text{Fe}(d, n)^{57}\text{Co}$ and $^{56}\text{Fe}(d, 2n)^{56}\text{Co}$ reactions [cf. 11] we estimated the impurity levels of ^{57}Co and ^{56}Co for various enrichments of ^{54}Fe . For an ^{54}Fe enrichment of 86% and the energy range $E_d = 10 \rightarrow 5$ MeV, the levels of ^{57}Co and ^{56}Co in ^{55}Co would amount to ~ 0.11 and 0.04%, respectively. In order to keep the level of long lived impurities below 0.1%, it is thus essential that ^{54}Fe enrichments lower than 90% are not used. The availability of high-purity ^{55}Co might lead to its use over more extended periods. The major difficulty with the $^{54}\text{Fe}(d, n)$ process, however, relates to targetry. On the one hand, the cost of enriched ^{54}Fe is rather high and, on the other, no high-current irradiation technique has been reported. To date the yields are limited to about 400 MBq. For a wider use of this production route, development of high-current targetry is absolutely necessary.

3. Cross section measurements

Detailed cross section measurements on the $^{54}\text{Fe}(d, n)^{55}\text{Co}$ and $^{54}\text{Fe}(d, \alpha)^{52g}\text{Mn}$ reactions have already been described [cf. 9 and references cited therein]. However, in that work the short-lived products formed via the $^{54}\text{Fe}(d, \alpha)^{52m}\text{Mn}$ and $^{54}\text{Fe}(d, t)^{53m,g}\text{Fe}$ processes were not investigated. There is some interest in investigating those products. The radionuclide ^{52m}Mn ($T_{1/2} = 21.1$ min; $E_{\beta^+} = 2.6$ MeV; $I_{\beta^+} = 97\%$; $E_{\gamma} = 1434.1$ keV; $I_{\gamma} = 98.2\%$) is potentially useful for PET studies on fast manganese uptake in an organ. The radioisotopes ^{53m}Fe ($T_{1/2} = 2.6$ min; $IT = 100\%$; $E_{\gamma} = 1328.2$ keV; $I_{\gamma} = 86.0\%$) and ^{53g}Fe ($T_{1/2} = 8.5$ min; $E_{\beta^+} = 2.8$ MeV; $I_{\beta^+} = 97\%$; $E_{\gamma} = 377.9$ keV; $I_{\gamma} = 42\%$) have relatively high nuclear spins (19/2 $^-$ and 7/2 $^-$, respectively). Their formation at a relatively low excitation energy is thus of fundamental interest.

As usual, cross sections were measured by the well-known stacked-foil technique. About 25 μm thick $^{\text{nat}}\text{Fe}$ foils were irradiated in the form of several stacks. The irradiation time in each case was 15 min and the radioactivity was determined non-destructively via high-resolution HPGe detector γ -ray spectrometry. The 8.5 min ^{53g}Fe was identi-

Table 2. Measured cross sections of some deuteron induced nuclear reactions.

Deuteron energy ^a (MeV)	Cross section (mb)	
	$^{54}\text{Fe}(d, \alpha)^{52\text{m}}\text{Mn}$	$^{54}\text{Fe}(d, t)^{53}\text{Fe}$
4.6 ± 0.5	8 ± 1.5	
6.0 ± 0.5	18 ± 3	
6.5 ± 0.5	20 ± 3	
7.2 ± 0.5	23 ± 3	
7.6 ± 0.4	26 ± 3	
8.8 ± 0.4	29 ± 3	
9.8 ± 0.4	33 ± 4	
10.3 ± 0.4	33 ± 4	
10.7 ± 0.4	34 ± 4	
11.2 ± 0.3	32 ± 4	0.17 ± 0.06
11.6 ± 0.3	30 ± 4	
12.1 ± 0.3	26 ± 3	0.28 ± 0.09
12.5 ± 0.3	26 ± 3	
13.1 ± 0.3	24 ± 3	0.36 ± 0.09
13.6 ± 0.3	22 ± 3	
13.8 ± 0.3	24 ± 3	0.49 ± 0.14

a: The deviation gives a quadratic sum of the primary energy error and the energy spread within a sample.

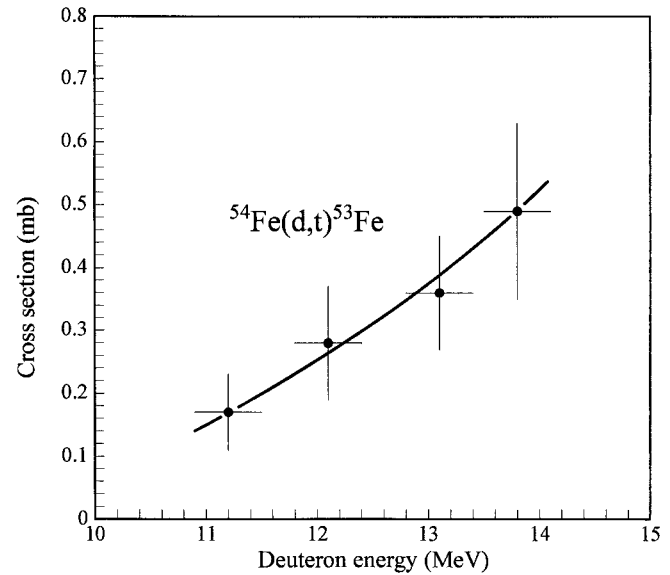
fied via the 377.9 keV γ -ray and the 21.1 min $^{52\text{m}}\text{Mn}$ via the 1434.1 keV γ -ray. Other techniques related to deuteron flux measurement, determination of absolute activity and calculation of cross section and its error were similar to those described earlier [9]. For deuteron beam monitoring the reaction $^{\text{nat}}\text{Fe}(d, xn)^{56}\text{Co}$ was used. Its cross sections were taken from a recent evaluation [12].

The results are given in Table 2 and have been corrected for the 5.8% abundance of ^{54}Fe in $^{\text{nat}}\text{Fe}$. At the deuteron energies involved in this work, reactions on the most abundant isotope ^{56}Fe cannot contribute to the formation of $^{52\text{m}}\text{Mn}$ and ^{53}Fe . Despite an intensive and careful γ -ray spectrometric analysis the very high-spin and short-lived $^{53\text{m}}\text{Fe}$ ($T_{1/2} = 2.6$ min) could not be identified. An upper limit for its formation cross section at $E_d = 13.8$ MeV was placed at 0.1 mb. Other results are discussed below.

3.1 $^{54}\text{Fe}(d, t)^{53}\text{Fe}$ reaction

The excitation function is shown in Fig. 1. The experimental threshold of the reaction is at about 10 MeV. As expected, the cross section increases with the increasing deuteron energy. The product could be formed, in principle, via three routes, viz. $^{54}\text{Fe}(d, p2n)^{53}\text{Fe}$, $^{54}\text{Fe}(d, dn)^{53}\text{Fe}$ and $^{54}\text{Fe}(d, t)^{53}\text{Fe}$ processes. The Q-values of those processes are -15.61, -13.38 and -7.12 MeV, respectively. It is therefore obvious that over the energy region considered here, the (d, t) process makes the largest contribution. Since the deuteron could easily pick up a neutron, the emission of the triton would presumably occur via a direct interaction process.

The formation of ^{53}Fe has been investigated in $^{54}\text{Fe}(p, pn)^{53}\text{Fe}$ [13], $^{54}\text{Fe}(n, 2n)^{53}\text{Fe}$ [14], $^{52}\text{Cr}(^3\text{He}, 2n)^{53}\text{Fe}$ [15] and $^{54}\text{Fe}(d, t)^{53}\text{Fe}$ [this work] processes. Their cross sections at an excitation energy of about 4 MeV above the respective threshold amount to 60, 70, 32 and 0.5 mb, respectively. The lowest value for the (d, t) reaction depicts that this process is intrinsically weak.

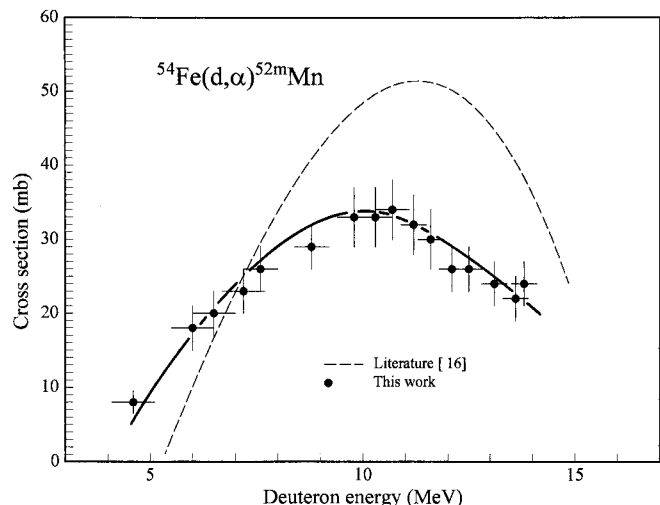
**Fig. 1.** Excitation function of the $^{54}\text{Fe}(d, t)^{53}\text{Fe}$ reaction. The solid line is an eye-guide.

3.2 $^{54}\text{Fe}(d, \alpha)^{52\text{m}}\text{Mn}$ reaction

The excitation function of this reaction is shown in Fig. 2. The threshold lies at about 4.0 MeV and the maximum at about 10.5 MeV. The shape of the curve is similar to those of other (d, α) reactions in this mass region. Clark *et al.* [16] had described a curve for this reaction; however, without giving any data points or errors. Their curve is reproduced in Fig. 2. We believe our data to be more accurate because of the use of improved experimental techniques, especially with regard to charged particle flux measurement and high-resolution γ -ray spectrometry.

3.3 Cross section ratios for the isomeric pair $^{52\text{m,g}}\text{Mn}$

Based on the cross sections of the $^{54}\text{Fe}(d, \alpha)^{52\text{g}}\text{Mn}$ reaction measured earlier [9] and the data for the $^{54}\text{Fe}(d, \alpha)^{52\text{m}}\text{Mn}$ reaction determined in this work, the ratio $\sigma_{\text{m}}/\sigma_{\text{g}}$ was cal-

**Fig. 2.** Excitation function of the $^{54}\text{Fe}(d, \alpha)^{52\text{m}}\text{Mn}$ reaction. The solid line is an eye-guide. The dashed line gives the results of Clark *et al.* [16].

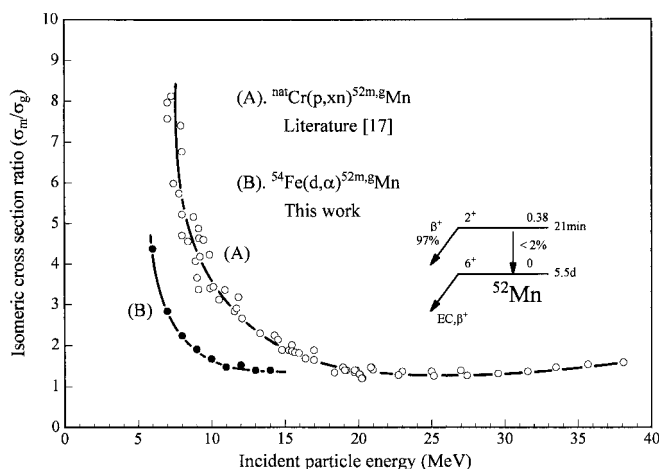


Fig. 3. Isomeric cross section ratio (σ_m/σ_g) in the reactions $^{nat}\text{Cr}(p, xn)^{52m,g}\text{Mn}$ and $^{54}\text{Fe}(d, \alpha)^{52m,g}\text{Mn}$ as a function of the respective projectile energy. The results for the former reaction have been taken from Klein *et al.* [17] and those for the latter reaction are based on an earlier [9] and present measurements. The solid lines are eye-guides.

culated and the results are shown in Fig. 3. Because of appreciable difference in the half-lives of the two isomers, measurements were done in two experiments, one involving short irradiations and the other longer irradiations. The ratio is high at low incident deuteron energies but decreases rapidly with the increasing energy. The trend is explainable in terms of the spins of the two states involved. The metastable state with a lower spin (2^+) is formed favourably at low incident projectile energies. The higher spin ground state (6^+) is more favoured at high projectile energies.

The σ_m/σ_g for the isomeric pair $^{52m,g}\text{Mn}$ has also been determined in the $^{nat}\text{Cr}(p, xn)^{52m,g}\text{Mn}$ processes [cf. 17], and the results are depicted in Fig. 3. Up to about 24 MeV only the $^{52}\text{Cr}(p, n)^{52m,g}\text{Mn}$ process is possible; at higher energies both this reaction and the $^{54}\text{Cr}(p, 3n)^{52m,g}\text{Mn}$ reaction contribute. There is a dramatic change in the ratio while proceeding from low to high incident energies. The trend is, however, the same as in the case of the (d, α) process. The spins of the two products involved and the incident projectile energy are thus the major deciding factors in the isomer distribution ratio; the type of reaction has some influence but it is not as important as the other two factors.

Acknowledgments. We thank Professor H. H. Coenen for his interest in this work. Our special thanks are due to the crew of the Compact Cyclotron CV 28 for many irradiations, the "Zentralabteilung für Chemische Analysen (ZCH)" for ICP-OES analysis of the Co-55 sample, and Messrs. K.-H. Linse, T. Manguay, C. Baltes and B. Reuß for their active participation in the production work. M.R.Z. is grateful to the Deutscher Akademischer Austauschdienst (DAAD) for the award of a senior fellowship and to the Rajshahi University for granting leave of absence.

References

- Lagunas-Solar, M. C., Jungermann, J. A.: Cyclotron production of carrier-free cobalt-55, a new positron emitting label for bleomycin. *Int. J. Appl. Radiat. Isot.* **30**, 25 (1979).
- Nieweg, O. E., Piers, D. A., Beekhuis, H., Paans, A. M. J., Welleweerd, J., Vaalburg, W., Woldring, M. G.: Co-55 bleomycin in the detection of lung cancer and brain metastases. *J. Nucl. Med.* **22**, 50 (1981).
- Srivastava, S. C., Mausner, L. F., Mease, R. C., Kolsky, K. L., Meinken, G. E., Joshi, V., Pyatt, B., Wolf, A. P., Schlyer, D. J., Levy, A. V., Fowler, J. S.: Co-55 labeled monoclonal antibodies (Mabs) for tumor imaging with PET. *J. Nucl. Med.* **34**, 237 (1993).
- Jansen, H. M. L., Pruim, J., v. d. Vliet, A. M., Paans, A. M. J., Hew, J. M., Franssen, E. J. F., de Jong, B. M., Kosterink, J. G. W., Haaxma, R., Korf, J.: Visualisation of damaged brain tissue after ischemic stroke with cobalt-55 positron emitting tomography. *J. Nucl. Med.* **35**, 456 (1994).
- Mazière, B., Stulz, O., Verret, J. M., Comar, D., Syrota, A.: [^{55}Co] and [^{64}Cu]DTPA: New radiopharmaceuticals for quantitative tomocisternography. *Int. J. Appl. Radiat. Isot.* **34**, 595 (1983).
- Reimer, P., Qaim, S. M.: Excitation functions of proton induced reactions on highly enriched ^{58}Ni with special relevance to the production of ^{55}Co and ^{57}Co . *Radiochim. Acta* **80**, 113 (1998).
- Spellerberg, S., Reimer, P., Blessing, G., Coenen, H. H., Qaim, S. M.: Production of ^{55}Co and ^{57}Co via proton induced reactions on highly enriched ^{58}Ni . *Appl. Radiat. Isot.* **49**, 1519 (1998).
- Sharma, H., Zweit, J., Smith, A. M., Downey, S.: Production of cobalt-55, a short-lived, positron emitting radiolabel for bleomycin. *Appl. Radiat. Isot.* **37**, 105 (1986).
- Zaman, M. R., Qaim, S. M.: Excitation functions of (d, n) and (d, α) reactions on ^{54}Fe : relevance to the production of high-purity ^{55}Co at a small cyclotron. *Radiochim. Acta* **75**, 59 (1996).
- Denzler, F.-O., Lebedev, N. A., Novgorodov, A. F., Rösch, F., Qaim, S. M.: Production and radiochemical separation of ^{147}Gd . *Appl. Radiat. Isot.* **48**, 319 (1997).
- Sudár, S., Qaim, S. M.: Excitation functions of proton and deuteron induced reactions on iron and alpha-particle induced reactions on manganese in the energy region up to 25 MeV. *Phys. Rev. C* **50**, 2408 (1994).
- Tarkányi, F., Tákács, S., Gul, K., Hermanne, A., Mustafa, M. G., Nortier, M., Oblozinsky, P., Qaim, S. M., Scholten, B., Shubin, Y. N., Zhuang Youxiang: Beam monitor reactions. In: *Charged particle cross section database for medical radioisotope production: diagnostic radioisotopes and monitor reactions*. IAEA-TECDOC-1211, Vienna (2001) pp. 107–110.
- Keller, K. A., Lange, J., Münzel, H., Pfennig, G.: *Excitation functions for charged-particle induced nuclear reactions*. Landolt-Börnstein Series Group I, Vol. 55, Springer Verlag, Berlin (1973) p. 188.
- Fessler, A.: Activation cross sections and isomeric cross section ratios in neutron induced reactions on Cr-, Fe- and Ni-isotopes in the energy range 9 to 21 MeV. *Forschungszentrum Jülich, Report JÜL-3502* (1998).
- Fessler, A., Alfassi, Z. B., Qaim, S. M.: Excitation functions of ^3He -particle induced nuclear reactions on natural chromium: Possibilities of production of ^{52}Fe , ^{53}Fe and ^{52}Mn for medical use. *Radiochim. Acta* **65**, 207 (1994).
- Clark, J. W., Fulmer, C. B., Williams, I. R.: Excitation functions for radioactive nuclides produced by deuteron induced reactions in iron. *Phys. Rev.* **179**, 1104 (1969).
- Klein, A. T. J., Rösch, F., Qaim, S. M.: Investigation of $^{50}\text{Cr}(d, n)^{51}\text{Mn}$ and $^{nat}\text{Cr}(p, x)^{51}\text{Mn}$ processes with respect to the production of the positron emitter ^{51}Mn . *Radiochim. Acta* **88**, 253 (2000).